Chapter 6

Biomaterial for Bone and Dental Implants: Synthesis of B-Type Carbonated Hydroxyapatite from Biogenic Source

Bernard Owusu Asimeng, David Walter Afeke and Elvis Kwason Tiburu

Abstract

There are several sources from which hydroxyapatite (HAp) can be obtained and may be broadly categorized as synthetic or biogenic. Elevated interest in recent times has pushed for the development of several procedures for extracting HAp from biogenic wastes due to their excellent composition and morphology resemblance to the human calcified tissue (B-type carbonated HAp). Notable biogenic sources reported for HAp extraction span bovine bones, fish scales, corals, eggshells, and snails among other calcium-rich sources. However, most of the synthetic methods are laborious and therefore result in high production costs. In this chapter, we discuss the synthesis of B-type carbonate substituted HAp from an untapped biogenic source, *Achatina achatina* shells, using a simple precipitation method and a controlled heat-treatment method. This unique treatment method affected the substitution resulting in different crystallographic parameters and revealed a novel material for bone implants and enamel applications.

Keywords: biogenic source, biomaterial, carbonated hydroxyapatite

1. Introduction

Hydroxyapatite (HAp) is a member of the calcium apatite (group of phosphate) family with a high concentration of hydroxyl group [1–3]. Stoichiometric HAp, $Ca_{10}(PO_4)_6(OH)_2$ can exhibit either monoclinic or hexagonal crystal structures [4, 5]. The most frequently reported hydroxyapatite crystal structure is the hexagonal system, which consists of unconnected, PO_4^{3-} tetrahedra with Ca^{2+} in the interstitial space and a chain of OH^- ions along the c-axis to balance the unit cell charges [4]. This hexagonal crystal structure allows for replacement (substitution) of ions into the structure. The substitution makes the HAp more reactive and biocompatible [6, 7]. The human calcified tissue (e.g., bone and tooth enamel) consists of mineral components similar to carbonated HAp (CHAp) [8, 9]. As a result, extensive research has been conducted to substitute carbonate into commercial HAp to achieve a suitable material for hard tissue replacement and implants coatings [10, 11].

There are two main types of carbonate (CO_3) substitution that occur in hydroxyapatite, namely A-type and B-type. A-type occurs when CO_3 replaces OH

groups, while B-type substitution occurs when CO_3 replaces PO_4 in the apatite structure. If these substitutions take place concurrently, an AB-type substitution occurs. Among the types of substitution, literature reports that B-type CHAp is highly similar to the human calcified tissue, which contains 3–5 wt% of carbonate in the lattice of the phosphate [12–15].

Laboratories have advanced in methods for the synthesis of B-type CHAp but the methods are laborious and expensive. For example, the method most frequently reported in the literature is the one proposed by LeGeros [16]. Herein, the preparation begins by adding PO_4/CO_3 solution in a stepwise manner into $Ca(NO_3)_2{\cdot}4H_2O$ solution at a temperature of 90°C. The mixture is stirred for 5 h at a pH of 11 and the precipitates filtered and dried for 10 h at 100°C in an oven. The B-type CHAp is then identified using X-ray diffractometry (XRD) and infra-red (IR) spectrometry. The XRD is a good analytical tool to study the substitution since; CO_3 has a smaller planar ion diameter than the tetrahedral PO_4 group, and thus the substitution of CO_3 with PO_4 will result in a decrease of the a-axis and a small increase in the c-axis of the unit cell. On the other hand, in a narrow range, vibrating bonds of functional groups in a material vibrate with a characteristic wavenumber [17], which is why IR spectroscopy is used to study the functional groups.

In this chapter, the authors discussed a simple precipitation and heat treatment method for the preparation of B-type CHAp from *Achatina achatina* (AA) shells and phosphate-containing solution. Additionally, the XRD and IR results obtained for the substitution are discussed.

2. Obtaining calcite from the AA shells for HAp preparation

Achatina achatina (AA) is the giant African snail ubiquitously scattered throughout the African continent particularly in West Africa, Ghana. The land strata of the soil are made up of various ions, and the eating habit of the snails enables the ingestion of these ions into their shells in trace amounts. The AA shells, however, serve as a rich source of calcium carbonate ($CaCO_3$)—a precursor for HAp preparation compared to other biogenic sources like bovine bones, fish scales, corals, eggshells, and other landmark snail shells. $CaCO_3$ mainly exists in two crystal forms: aragonite and calcite. The aragonite structure as indicated by the XRD pattern in **Figure 1(a)** exists in 'raw ground' AA shells after the shells are washed with running water to remove sludge and dried in the open air for 6 h. The structure contains impurities like sulphate (SO_4^{2-}) and is indicated in the IR spectra in **Figure 2(a)**. These impurities consequently rule out raw AA powders as carbonate precursors for the HAp formation. Thus, the raw AA powder is calcined at high temperatures to burn the impurities and convert the aragonite structure into calcite. The calcination temperature typically used is between 600 and 800°C [18] [see **Figure 1(b)**–**(d)**]. The IR spectra in **Figure 2(b)** and **(c)** support XRD patterns, which show that the temperatures (600 and 700°C) facilitate the conversion of the aragonite structure to calcite. The calcite functional groups occur at wavenumbers 712, 856, and 1418 cm^{-1}. The calcite structure is formed at the two temperatures, however, the ideal calcination temperature for HAp synthesis is between 800 and 850°C. These temperatures bring an additional phase to the calcite to initiate the HAp preparation. The evidence is shown in **Figure 2(d)** where a dual-phase of calcite and calcium hydroxide [$Ca(OH)_2$] is observed. The calcite absorbed moisture from the atmosphere during the open-air drying; so, under high temperature (800°C) the $CaCO_3$ decomposes to form $Ca(OH)_2$. The reaction pathway is given by **Eqs. (1)** and **(2)**:

$$CaCO_3 + H_2O \xrightarrow{heat(800°C)} CaO.H_2O + CO_2\uparrow \quad (1)$$

$$CaO.H_2O \rightarrow Ca(OH)_2 \quad (2)$$

The reaction is confirmed with IR results in **Figure 2(d)** showing the hydroxyl group (OH^-) of calcium hydroxide at wavenumber 3642 cm^{-1}, and calcium oxide (Ca—O bonding) stretches from wavenumbers 400 to 700 cm^{-1} in calcite.

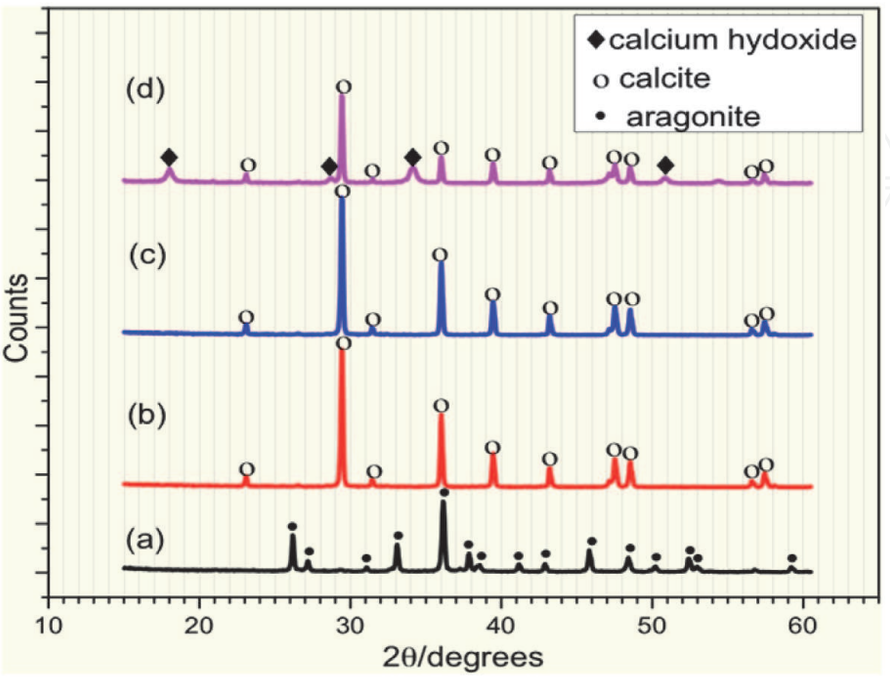

Figure 1.
XRD patterns of (a) raw uncalcined AA powder and (b) calcined AA powder at 600°C (c) 700°C (d) 800°C.

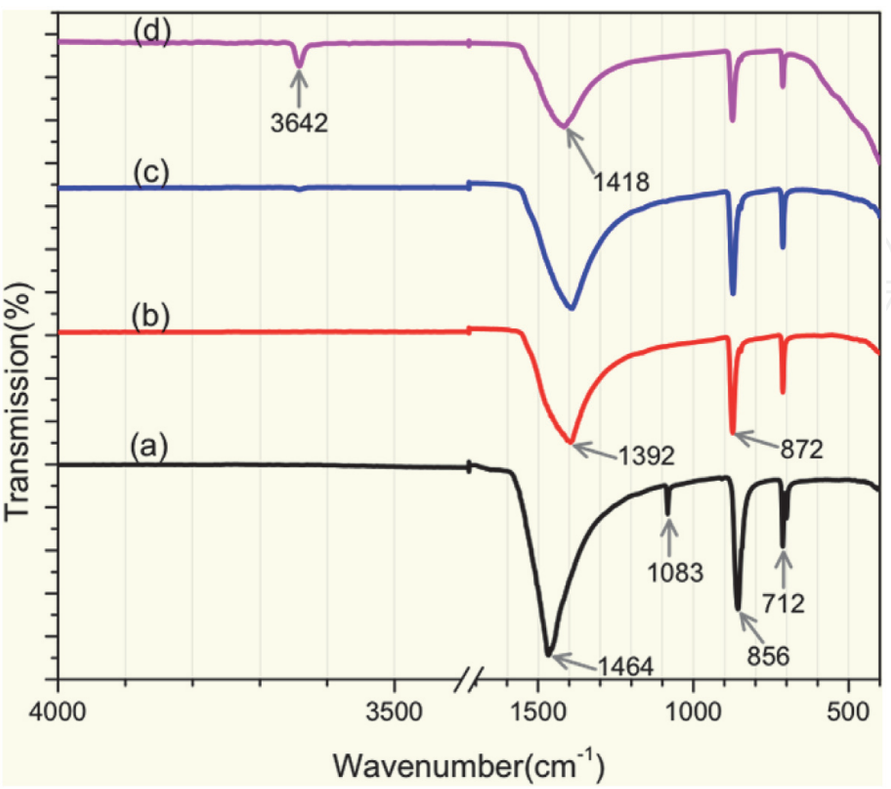

Figure 2.
IR spectra of (a) raw uncalcined AA powder and (b) calcined AA powder at 600°C (c) 700°C and (d) 800°C.

3. HAp preparation

HAp is prepared from 0.3 M solution of diammonium hydrogen phosphate (DHP, pH of 8.12) and 5.7 g of calcite. The calcite is dissolved in distilled water of volume 0.15 cm^3 and the same volume of calcite is measured for DHP. The DHP is then added stepwise while stirring at 40°C for 1 h. The stirring time controls the particle size. The longer the stirring time the smaller the particle size [14]. The calcite mostly preferred for HAp preparation has $Ca(OH)_2$ phase; so, in aqueous solution, the $Ca(OH)_2$ quickly dissociates into $2Ca^{2+}$ and $2OH^-$, whereas $(NH_4)_2HPO_4$ produces $(NH_4)_2OH$ and a monophosphoric acid (HPO_4). The monophosphoric acid reacts with OH groups released by the calcium hydroxide to form a phosphate ester through a condensation reaction. The phosphate ester reacts with Ca to form HAp. The reaction is allowed to age for 24 h to enable HAp crystals growth [14]. The ammonium hydroxide is filtered together with water to obtain the HAp crystals. The reaction pathway is given in Eq. (3):

$$10Ca(OH)_2 + 6(NH_4)_2.HPO_4 + 2H_2O \rightarrow Ca_{10}(PO_4)_6(OH)_2 + 12NH_4OH_{(l)} + 8H_2O \quad (3)$$

4. B-type carbonated HAp preparation

The calcite ($CaCO_3$) in the mixed-phase of the HAp precursor decomposes into calcium (Ca^{2+}) and carbonate (CO_3^{2-}) during stirring. The calcium is used as part of the HAp formation and the CO_3^{2-} lies behind the lattice of phosphate (PO_4^{3-}). The ionic diameter of PO_4^{3-} is larger than that of CO_3^{2-}, thus the first masked the latter and is not detected using XRD. The IR spectra in **Figure 3(a)** show major functional groups of HAp and minor functional groups of carbonate. The PO_4^{3-} groups of HAp

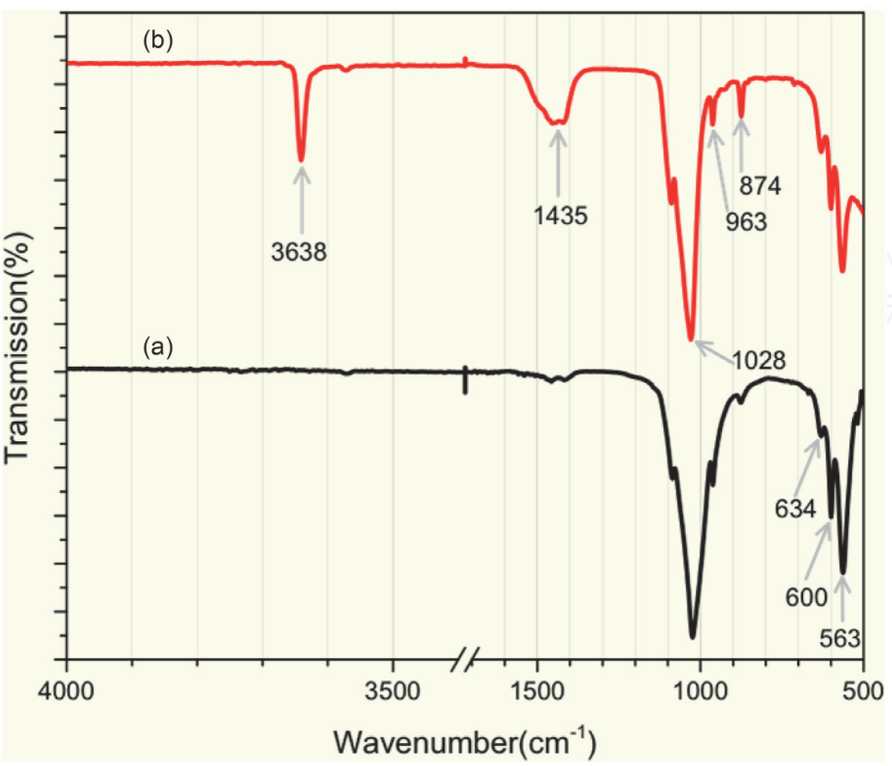

Figure 3.
IR spectra of (a) HAp without heat treatment and (b) HAp with heat treatment at 850°C. The figure is obtained from Asimeng et al.

occur at wavenumbers 1028, 963, 600, and 563 cm^{-1} whereas CO_3^{2-} groups are found at 1435 and 874 cm^{-1}. The HAp is subjected to a temperature of 850°C for 12 h for annealing and normalizing. The heat treatment initiates the substitution of CO_3^{2-} for PO_4^{3-} as indicated in Eq. (4). **Figure 3(b)** shows functional groups of the heat-treated HAp. The CO_3^{2-} groups at 1435 cm^{-1} are now prominent and the OH^- groups, which are absent in HAp without heat treatment, are also intense, which serves as evidence of B-type carbonate HAp.

$$Ca_{10-\frac{x}{2}}(PO_4)_{6-x}(OH)_2 + CO_{3x} \xrightarrow{heattreatment} Ca_{9.5}(PO_4)_5CO_3(OH)_2 \quad (4)$$

5. Discussion

Natural sources for hydroxyapatite synthesis have generated a lot of interest in recent times due to the various advantages it presents over synthetic sources in terms of similarity to the biological apatite (bone and dental). Some of these sources include but are not limited to plants, bovine bone, eggshells, and snail shells. All these biogenic sources have calcium carbonate as a precursor for HAp synthesis. Plant and algae, however, do not have a lot of calcium carbonate as compared to the other sources like bovine, eggshells, and snail shells [19]. The extraction of HAp, therefore, becomes somewhat laborious as there is the need for the addition of more calcium and/or phosphate precursors. This complicated process and the usage of additional calcium or phosphate source increases the cost of production. Clearly, this relegates plant and algae as a great source of HAp for biomedical applications. Biogenic sources such as seashells are rich in $CaCO_3$, however, due to their aquatic nature, they require additional processes/treatment to transform them into a pure phase of HAp [20]. The employment of a combination of extraction methods to achieve the transformation affects the cost of production greatly.

The increasing consumption of snails (Achatina sp.) as a delicacy across all of West Africa has caused a significant increase in snail shell waste production. The recovery of these shells allows for HAp synthesis and reduction in solid wastes. It is recorded in the literature that eggshells and snail shells have a lot of calcium carbonate but the percentage composition in snail shells is more than in eggshells [21]. Snail shells are reported to have about 95–99% calcium carbonate [21]. Bovine bones, comparable to snail shells, present excellent properties to extract HAp but using bovine bones would require a processing technique (hydrothermal process), which is very expensive.

Several extraction methods have been documented for the synthesis of HAp. These fabrication methods include dry methods (solid-state and mechanochemical), wet methods (chemical precipitation, hydrolysis, sol-gel, hydrothermal, emulsion, and sonochemical), and high-temperature processes (combustion and pyrolysis) [22]. It is mostly reported in the literature that wet chemical precipitation tops the chart when it comes to cost-effectiveness considering the materials used and their availability. Also, the use of the wet chemical precipitation method typically results in a low crystalline material compared to a hydrothermally extracted HAp. According to ISO 23317, calcium apatite similar to the bone or enamel apatite should be Ca-deficient and made up of impurities such as CO_3^{2-} and Na^+ and have low crystallinity. It should be noted that for biomedical applications, one desirable property is nano-sized particles. The extraction of nano-sized HAp has advantages in terms of high surface activity and ultrafine structures [23–25], higher bioactivity, and better resorbability than micron-sized particles. With this in mind, the author

Properties	Mammalian (bovine bone, porcine bone, horse bone, camel bone)	Aquatic/marine (fish scales, fish bone)	Other shells (cockle shell, clam, sea shell, eggshell)	Plant/algae	AA shell
Morphology	Irregular, rod-like, flakelike, needle-like, plate-like	Flat-plate, hexagonal, rod-like, irregular, nearly spherical, agglomerate, vary	Spherical, needle-like, rod like, globules, agglomerate polygonal	Flakes, cluster, rectangular, elongate	Needle-like, rod like, spheroids
Particle size	20 nm–500 μm	5 nm–1.0 μm	5 nm–10.4 μm	50–500 nm	12–17 nm
Crystallinity	High (calcination) Low (chemical treatment)	High (calcination) Low (chemical treatment)	High (combination method) Low (chemical treatment)	High (calcination) Low (chemical treatment)	78.2–83.32%
Crystalline Phases	HAp, β-TCP, CaO	HAp, β-TCP, TCP	HAp, calcite, βTCP	HAp þ whitlockite, $CaCO_3$, βTCP, SiO_2	HAp, calcite
References	[26–30]	[31–36]	[37–41]	[42–46]	Asimeng et al.

Table 1.
A summary of the properties of HAp from different biogenic sources.

has successfully extracted HAp from AA shells with particle size in the nanosize range in his previous works. Also, it should be noted that results of an earlier work conducted by Asimeng et al. on the extraction of HAp from the AA shells highlight particle size, lattice parameters, physiochemical properties, and morphological characteristics typical of the human enamel apatite. HAp obtained from the AA shells has further been subjected to a heat treatment to obtain a B-type carbonated HAp and this has significantly improved the physicochemical properties for applications in dentistry and orthopedics. The unit cell parameters of HAp with and without heat treatment are reported by Asimeng et al. The crystallographic information of the B-type carbonated HAp supports the theory that the unit cell a-axis decreases whereas c-axis increases as compared to the HAp without heat treatment.

Table 1 provides a comparative summary of properties of HAp extracted from the different sources and AA shell.

6. Conclusion

This book chapter discussed the synthesis of heat-treated B-type carbonated hydroxyapatite (CHAp) from *Achatina achatina* snail shells and diammonium hydrogen phosphate (DHP) for human calcified tissue replacement and coatings. The synthesis process is in three steps: [1] conversion of the shell crystal structure from aragonite to calcite, [2] precipitation of calcite and DHP to form hydroxyapatite (HAp), and [3] annealing and normalizing the HAp to form B-type CHAp. The synthesis reveals that calcination temperature plays a key role in step [1]. It was noticed that temperatures from 800 to 850°C provided an additional phase (calcium hydroxide) that is required to produce hydroxyl groups for the phosphoric ester

formation needed for the HAp synthesis. Also, it is recorded herein that heat treatment facilitated the substitution of CO_3^{2-}.

Acknowledgements

The authors acknowledge Mr. Osman Wahidu and Mr. Richard Asiamah for the support provided during material synthesis.

Author details

Bernard Owusu Asimeng*, David Walter Afeke and Elvis Kwason Tiburu
Department of Biomedical Engineering, University of Ghana, Legon, Ghana

*Address all correspondence to: boasimeng@ug.edu.gh

References

[1] Kannan S, Ventura JM, Ferreira JMF. In situ formation and characterization of flourine-substituted biphasic calcium phosphate ceramics of varied F-HAP/β-TCP ratios. Chemistry of Materials. 2005;**17**(12):3065-3068

[2] Chavan PN, Bahir MM, Mene RU, Mahabole MP, Khairnar RS. Study of nanobiomaterial hydroxyapatite in simulated body fluid: Formation and growth of apatite. Materials Science and Engineering B. 2010;**168**(1):224-230. DOI: 10.1016/j.mseb.2009.11.012

[3] Hui J, Li H, Zheng X, Ma H, Fan D, Liu H, et al. Control synthesis and self-assembly of calcium apatite at low temperatures. Ceramics International [Internet]. 2015;**41**(5):6194-6202. DOI: 10.1016/j.ceramint.2014.12.156

[4] Šimková L, Gorodylova N, Dohnalová Ž, Šulcová P. Influence of precipitation conditions on the synthesis of hydroxyapatite. Ceramics-Silikáty. 2018;**62**(3):253-260

[5] Tayyebi S, Mirjalili F, Samadi H, Nemati A. A review of synthesis and properties of hydroxyapatite / alumina Nano composite powder. Chemistry Journal. 2015;**05**(2):20-28

[6] Yashima M, Yonehara Y, Fujimori H. Experimental visualization of chemical bonding and structural disorder in hydroxyapatite through charge and nuclear-density analysis. Journal of Physical Chemistry C. 2011;**115**(50): 25077-25087

[7] Tank KP, Sharma P, Kanchan DK, Joshi MJ. FTIR, powder XRD, TEM and dielectric studies of pure and zinc doped nano-hydroxyapatite. Crystal Research and Technology. 2011;**46**(12):1309-1316

[8] Dorozhkin SV, Epple M. Biological and medical significance of calcium phosphates. Angewandte Chemie, International Edition. 2002;**41**(12): 3130-3146

[9] Barralet J, Best S, Bonfield W. Carbonate substitution in precipitated hydroxyapatite: An investigation into the effects of reaction temperature and bicarbonate ion concentration. Journal of Biomedical Materials Research. 1998; **41**(1):79-86

[10] Astala R, Stott MJ. First principles investigation of mineral component of bone: CO3 substitutions in hydroxyapatite. Chemistry of Materials. 2005;**17**(16):4125-4133

[11] Landi E, Tampieri A, Mattioli-Belmonte M, Celotti G, Sandri M, Gigante A, et al. Biomimetic Mg- and Mg,CO3-substituted hydroxyapatites: Synthesis characterization and in vitro behaviour. Journal of the European Ceramic Society. 2006;**26**(13): 2593-2601

[12] Ren F, Leng Y. Carbonated apatite, type-a or type-B? Key Engineering Materials. 2012;**493**:293-297

[13] LeGeros RZ. Properties of osteoconductive biomaterials: Calcium phosphates. Clinical Orthopaedics and Related Research. 2002;**395**:81-98

[14] Asimeng BO, Fianko JR, Kaufmann EE, Tiburu EK, Hayford CF, Anani PA, et al. Preparation and characterization of hydroxyapatite from Achatina achatina snail shells: Effect of carbonate substitution and trace elements on defluoridation of water. Journal of Asian Ceramic Societies. 2018;**6**(3):205-212

[15] Madupalli H, Pavan B, Tecklenburg MMJ. Carbonate substitution in the mineral component of bone: Discriminating the structural changes, simultaneously imposed by carbonate in a and B sites of apatite.

Journal of Solid State Chemistry. 2017; **255**:27-35

[16] Zapanta-Legeros R. Effect of carbonate on the lattice parameters of apatite. Nature. 1965;**206**(4982):403-404

[17] Coates J. Interpretation of infrared spectra, a practical approach. Encyclopedia of Analytical Chemistry: Applications, Theory and Instrumentation. 2006

[18] Akram M, Ahmed R, Shakir I, Ibrahim WAW, Hussain R. Extracting hydroxyapatite and its precursors from natural resources. Journal of Materials Science. 2014;**49**(4):1461-1475

[19] Oladele IO, Agbabiaka OG, Olasunkanmi OG, Balogun AO, Popoola MO. Non-synthetic sources for the development of hydroxyapatite. Journal of Applied Biotechnology & Bioengineering. 2018;**5**:92-99

[20] Mohd Pu'ad NAS, Koshy P, Abdullah HZ, Idris MI, Lee TC. Syntheses of hydroxyapatite from natural sources. Heliyon. 2019;**5**(5): e01588

[21] White MM, Chejlava M, Fried B, Sherma J. The concentration of calcium carbonate in shells of freshwater snails. American Malacological Bulletin. 2007; **22**(1):139-142

[22] Zhang X, Vecchio KS. Hydrothermal synthesis of hydroxyapatite rods. Journal of Crystal Growth. 2007;**308**(1): 133-140

[23] Vallet-Regí M, González-Calbet JM. Calcium phosphates as substitution of bone tissues. Progress in Solid State Chemistry. 2004;**32**(1–2):1-31

[24] Cai Y, Liu Y, Yan W, Hu Q, Tao J, Zhang M, et al. Role of hydroxyapatite nanoparticle size in bone cell proliferation. Journal of Materials Chemistry. 2007;**17**(36):3780-3787

[25] Wang J, Burken JG, Zhang XJ. Effect of seeding materials and mixing strength on Struvite precipitation. Water Environment Research. 2006; **78**(2):125-132

[26] Ayatollahi MR, Yahya MY, Asgharzadeh Shirazi H, Hassan SA. Mechanical and tribological properties of hydroxyapatite nanoparticles extracted from natural bovine bone and the bone cement developed by nano-sized bovine hydroxyapatite filler. Ceramics International. 2015;**41**(9): 10818-10827

[27] Ruksudjarit A, Pengpat K, Rujijanagul G, Tunkasiri T. Synthesis and characterization of nanocrystalline hydroxyapatite from natural bovine bone. Current Applied Physics. 2008;**8** (3–4):270-272

[28] Barakat NAM, Khil MS, Omran AM, Sheikh FA, Kim HY. Extraction of pure natural hydroxyapatite from the bovine bones bio waste by three different methods. Journal of Materials Processing Technology. 2009;**209**(7): 3408-3415

[29] Hosseinzadeh E, Davarpanah M, Nemati NH, Tavakoli SA. Fabrication of a hard tissue replacement using natural hydroxyapatite derived from bovine bones by thermal decomposition method. International Journal of Organ Transplantation Medicine. 2014;**5**(1):23

[30] Sun RX, Lv Y, Niu YR, Zhao XH, Cao DS, Tang J, et al. Physicochemical and biological properties of bovine-derived porous hydroxyapatite/collagen composite and its hydroxyapatite powders. Ceramics International [Internet]. 2017;**43**(18):16792-16798. DOI: 10.1016/j.ceramint.2017.09.075

[31] Paul S, Pal A, Choudhury AR, Bodhak S, Balla VK, Sinha A, et al. Effect of trace elements on the sintering effect of fish scale derived hydroxyapatite and its bioactivity.

Ceramics International. 2017;**43**(17): 15678-15684

[32] Pal A, Paul S, Choudhury AR, Balla VK, Das M, Sinha A. Synthesis of hydroxyapatite from lates calcarifer fish bone for biomedical applications. Materials Letters. 2017;**203**:89-92

[33] Sunil BR, Jagannatham M. Producing hydroxyapatite from fish bones by heat treatment. Materials Letters. 2016;**185**:411-414

[34] Pon-On W, Suntornsaratoon P, Charoenphandhu N, Thongbunchoo J, Krishnamra N, Tang IM. Hydroxyapatite from fish scale for potential use as bone scaffold or regenerative material. Materials Science and Engineering: C. 2016;**62**:183-189

[35] Kongsri S, Janpradit K, Buapa K, Techawongstien S, Chanthai S. Nanocrystalline hydroxyapatite from fish scale waste: Preparation, characterization and application for selenium adsorption in aqueous solution. Chemical Engineering Journal. 2013;**215**:522-532

[36] Venkatesan J, Qian ZJ, Ryu B, Thomas NV, Kim SK. A comparative study of thermal calcination and an alkaline hydrolysis method in the isolation of hydroxyapatite from Thunnus obesus bone. Biomedical Materials. 2011;**6**(3):035003

[37] Mustaffa R, Mohd Yusof MR, Abdullah Y. A novelty of synthetic hydroxyapatite from cockle shell and characterization. Advances in Materials Research. 2015;**1087**:429-433

[38] Santhosh S, Balasivanandha PS. Thermal stability of nano hydroxyapatite synthesized from sea shells through wet chemical synthesis. Materials Letters. 2013;**19**:121-124

[39] Mohamad Razali NAI, Pramanik S, Abu Osman NA, Radzi Z, Pingguan-Murphy B. Conversion of calcite from cockle shells to bioactive nanorod hydroxyapatite for biomedical applications. Journal of Ceramic Processing Research. 2016;**17**:699-706

[40] Pal A, Maity S, Chabri S, Bera S, Chowdhury AR, Das M, et al. Mechanochemical synthesis of nanocrystalline hydroxyapatite from Mercenaria clam shells and phosphoric acid. Biomedical Physics & Engineering Express. 2017;**3**(1):015010

[41] Goloshchapov DL, Kashkarov VM, Rumyantseva NA, Seredin PV, Lenshin AS, Agapov BL, et al. Synthesis of nanocrystalline hydroxyapatite by precipitation using hen's eggshell. Ceramics International. 2013;**39**(4): 4539-4549

[42] Govindaraj D, Rajan M. Synthesis and spectral characterization of novel nano-hydroxyapatite from Moringaoleifera leaves. Materials Today: Proceedings. 2016;**3**(6):2394-2398

[43] Tampieri A, Sprio S, Ruffini A, Celotti G, Lesci IG, Roveri N. From wood to bone: Multi-step process to convert wood hierarchical structures into biomimetic hydroxyapatite scaffolds for bone tissue engineering. Journal of Materials Chemistry. 2009; **12**(28):4973-4980

[44] Monballiu A, Desmidt E, Ghyselbrecht K, Meesschaert B. Phosphate recovery as hydroxyapatite from nitrified UASB effluent at neutral pH in a CSTR. Journal of Environmental Chemical Engineering. 2018;**6**(4): 4413-4422

[45] Teymouri A, Stuart BJ, Kumar S. Hydroxyapatite and dittmarite precipitation from algae hydrolysate. Algal Research. 2018;**29**:202-211

[46] Tsuru K, Ruslin, Maruta M, Matsuya S, Ishikawa K. Effects of the method of apatite seed crystals addition on setting reaction of α-tricalcium phosphate based apatite cement. Journal of Materials Science. Materials in Medicine. 2015;**26**(10):244